

Corresponding author:

Dr. Hongjian Feng

School of Science, Tianjin Polytechnic University, Tianjin 300160, China

Department of Physics and Astronomy, University of Missouri, Columbia, MO
65211, USA

Email address:

fenghongjian@gmail.com

fenghongjian1978@gmail.com

The role of Coulomb and exchange interaction on the Dzyaloshinskii-Moriya interaction(DMI) in BiFeO_3

Hongjian Feng^{a,b}

^a*School of Science, Tianjin Polytechnic University, Tianjin 300160, China*

^b*Department of Physics and Astronomy, University of Missouri, Columbia, MO
65211, USA*

Abstract

Ab initio calculations show that the Dzyaloshinskii-Moriya interaction(DMI) and net magnetization per unit cell in BiFeO_3 are reduced when U is increasing from 0 to 2.9 eV, and independent of J . Interestingly, the DMI is even destroyed as U exceeds a critical value of 2.9 eV. We propose a simple model to explain this phenomenon and present the nature of the rotation of the magnetization corresponding to altered antiferrodistortive distortions under DMI in BiFeO_3 .

Key words: Dzyaloshinskii-Moriya interaction(DMI); Multiferroics ;Density functional theory

PACS: 75.30.Et, 75.30.GW, 71.15.Mb

Email address: fenghongjian@gmail.com (Hongjian Feng).

1 Introduction

Multiferroic materials have attracted much interest due to the coexistence of magnetic and ferroelectric ordering in single phase. The coupling of the two ordering leads to the so-called magnetoelectric effect in which the magnetization can be tuned by the external electric field, and vice versa[1,2,3,4,5]. These materials have potential applications in information storage, the emerging field of spintronics, and sensors. BiFeO_3 is the rare one in nature, which possess both weak ferromagnetism and ferroelectric characteristics in single phase[6,7,8,9]. It has long been known to be ferroelectric with a Curie temperature of about 1103 K and antiferromagnetic (AFM) with a Néel temperature of 643 K. The Fe magnetic moments are coupled ferromagnetically in (1 1 1) plane and antiferromagnetically in the adjacent plane along [111] direction, which is known as the G-type AFM order. The rhombohedral distorted perovskite structure with space group $R3c$ permits a canting of AFM sublattice caused by the antisymmetric Dzyaloshinskii-Moriya interaction (DMI), resulting in a weak ferromagnetism. However, there is a spiral spin structure in which the AFM axis rotates through the crystal with a long-wavelength period of 620\AA . The cancellation of magnetization should be suppressed partly in thin film [6], or by partly substitution of magnetic transitional metal ions in B sites, as shown in our previous report[10]. It is known that the ferroelectricity in BiFeO_3 is produced by the lone Bi-6s stereochemically active pair induced by the mixing between the $(ns)^2$ ground state and a low-lying $(ns)^1(np)^1$ excited state, which can only occur if the cation ionic site does not have inversion symmetry, while the weak ferromagnetism is mainly attributed to Fe^{3+} ions. Therefore the coupling between the electric and the magnetic ordering becomes weak in BiFeO_3 , which agrees with the fact of large difference between the Curie temperature and AFM Néel temperature. There exists another structural distortion, so-

called antiferrodistortive(AFD) distortion, which is formed by the alternating sense of rotation of the oxygen octahedra along $[1\ 1\ 1]$ direction[11]. In our previous paper, we have shown that the rotation of the oxygen octahedra couples with the weak ferromagnetism due to the DMI, using *Ab initio* calculations with considering the spin-orbital(SO) coupling effect and the noncollinear spin configuration[12]. In strongly correlated materials, e.g. multiferroics, the on-site Coulomb(U) and exchange interaction(J) has been proposed to properly describe the partly filled localized d orbitals within density functional theory(DFT). One may wonder whether U and J will have an impact on the magnetization through DMI taking into account SO interaction. How do these parameters influence the DMI, and further the magnetization? What is the origin of coupling between the rotation of oxygen octahedra and the resulting magnetization in terms of DMI in BiFeO_3 ? In this paper we have proposed a transparent physical interpretation for the abovementioned questions, using first-principles calculations based on the DFT.

The remainder of this article is structured as follows: In section 2, we presented the computational details of our calculations. We provided the calculated results and discussions in section 3. In section 4, the conclusion based on our calculation were given.

2 Computational details

Our calculations were performed within the local spin density approximation(LSDA) to DFT using the ABINIT package[13,14]. The ion-electron interaction was modeled by the projector augmented wave (PAW) potentials [15,16] with a uniform energy cutoff of 500 eV. Bi 5d, 6s, and 6p electrons, Fe 4s, 4p, and 3d electrons, and O 2s and 2p electrons were considered as valence

states. Two partial waves per l quantum number were used. The cutoff radii for the partial waves for Bi, Fe, and O were 2.5, 2.3, 1.1 a.u., respectively. $6 \times 6 \times 6$ Monkhorst-Pack sampling of the Brillouin zone were used for all calculations. We calculated the net magnetization per unit cell and the electronic properties within the LSDA+U method where the strong coulomb repulsion between localized d states has been considered by adding a Hubbard-like term to the effective potential[17,18,19]. The effective Hubbard parameter, the difference between the Hubbard parameter U and the exchange interaction J ($U - J$), was changing in the range between 0 and 6 eV for the Fe d states. For the same value of ($U - J$), J was varying as 0, 0.5, 0.8, and 1 eV, respectively. Taking into account the SO interaction, we introduced the noncollinear spin configuration to construct the G-type AFM magnetic order with the AFM axis being along the x axis in Cartesian coordinates in our *Ab initio* calculation.

3 Results and discussion

In ref. 20 the author suggest that the inversion centers between adjacent B sites in ABO_3 perovskite structure are destroyed by the displacement of the oxygen anions located at the midpoints between them, while the space inversion centers between A sites still remains. Therefore ABO_3 structure with magnetic ions in A sites, such as $FeTiO_3$, should possess a strong coupling between the ferroelectric distortions and magnetization. It can not be achieved in ABO_3 structure with magnetic ions in B sites, such as $BiFeO_3$. That is to say the coupling between the ferroelectric distortions and magnetization in it shall be neglected. However in $BiFeO_3$ there exists another kind displacement, known as antiferrodistortive (AFD) distortions, caused by the rotation of the neighboring oxygen octahedra. Through antisymmetric superexchange interaction this AFD displacement couples weakly to the magnetization. In

this paper we mainly concentrate on the coupling associated with the DMI between the AFD distortions and the magnetization per unit cell.

For the AFD motion, a rotational vector \mathbf{R} has been introduced to describe the direction of the rotation of the oxygen octahedra[12]. From Fig. 1, the anticlockwise rotation of upper oxygen octahedra and clockwise rotation of lower oxygen octahedra correspond to the outward state defined as \mathbf{R}_{out} . The opposite state is defined as \mathbf{R}_{in} . The rotational angle is 10° in the Cartesian coordinates[12].

In our LSDA+U calculation, U and J are defined as

$$U = \frac{1}{(2l+1)^2} \sum_{m,m'} \langle m, m' | V_{ee} | m, m' \rangle = F^0, \quad (1)$$

$$J = \frac{1}{2l(2l+1)} \sum_{m \neq m', m'} \langle m, m' | V_{ee} | m, m' \rangle = \frac{F^2 + F^4}{14}, \quad (2)$$

where V_{ee} are the screened Coulomb interaction among the nl electrons. F^0 , F^2 , and F^4 are the radial Slater integrals for d electrons in Fe.

The net magnetization per unit cell with respect to \mathbf{R}_{in} and \mathbf{R}_{out} in Cartesian coordinates for different U and J were listed in table 1. It can be seen that J value have no effect on the resulting magnetization when U remains constant. For the sake of clarity, only the results obtained with different J value for $U=0$ and 2.9 eV were given in the table. The AFM vector in Cartesian coordinates with varying effective Hubbard U were illustrated in Fig. 2, where $[1\ 1\ 1]$ direction is taken as the z axis as shown schematically in Fig. 3, and the x, y , and z component of the magnetization is denoted by M_x , M_y , and M_z in the coordinates, respectively. Fig. 3 shows the coupling between the rotation of oxygen octahedra and the resulting magnetization per unit cell. The arrow indicate the spin direction of Fe for different states. The upper section corresponds to the \mathbf{R}_{in} rotational state, and lower section, the \mathbf{R}_{out}

rotational state. M_{total} is the net magnetization per unit cell. The dashed line arrow is the unstable rotational state. $[1\ 1\ 1]$ crystal direction is selected as the z axis, and the AFM order is arranged along x axis. It is clearly shown that the easy axis of the magnetization is y axis when G-type AFM order is arranged along the x axis, taking into account the SO interaction and the unconstrained freedom of spin. The antisymmetric interaction of the neighboring Fe1 and Fe2 ions leads to the canting of the magnetic moment of them away from their original direction (x axis) and a resulting magnetization mainly in y axis, which arises from the DMI only occurring when the inversion symmetry is broken. As U is approaching from 0 eV to 2.9 eV, the net magnetization is reversed by the opposite rotation of the oxygen octahedra in terms of the reversal of M_y , and decreases with increasing of U . However, M_y does not change sign with the altered AFD motion when U exceeds a critical value of 2.9 eV, say 3 eV, implying that the net magnetization only deviates slightly from the original direction and does not experience a significant rotational angle greater than 90° . As U attain to be the critical value, the DMI caused by the antisymmetric superexchange interaction is eliminated with the strong on-site Coulomb interaction. The AFD distortions do not couple with the magnetization.

In order to obtain an unambiguous interpretation for the effect of Coulomb and exchange interaction on the net magnetization, we need to recap the DMI on the coupling of neighboring Fe1 and Fe2 sites. We have for the interaction of neighboring Fe1 and Fe2 sites by the second order perturbation calculation[21,22,23]

$$E_{Fe1,Fe2}^{(2)} = \mathbf{J}_{Fe1,Fe2}^{(2)}(\mathbf{S}_1 \cdot \mathbf{S}_2) + \mathbf{D}_{Fe1,Fe2}^{(2)}(\mathbf{S}_1 \times \mathbf{S}_2) + \mathbf{S}(R) \cdot \Gamma_{Fe1,Fe2}^{(2)} \cdot \mathbf{S}_2. \quad (3)$$

The first term on the right hand side of the Eq. (3) corresponds to the usual isotropic superexchange interaction, and the second term is the DMI. Provided the long range pseudodipolar interaction is neglected, we get the Hamiltonian for the system

$$H_{BiFeO_3} = -2 \sum_{\langle 1i,2j \rangle} \mathbf{J}_{1i,2j} \mathbf{S}_{1i} \cdot \mathbf{S}_{2j} + \sum_{\langle 1i,2j \rangle} \mathbf{D}_{1i,2j} \mathbf{S}_{1i} \times \mathbf{S}_{2j}. \quad (4)$$

The first term comes from the symmetric superexchange, and the second one is the antisymmetric DMI contribution. $\mathbf{J}_{1i,2j}$ in the first term is a constant similar to the exchange interaction, and does not contribute to the DMI. This can account well for our calculated results that the exchange parameter J has nearly no effect on the rotation of the magnetization. \mathbf{D} is the DMI constant associated with the crystal field and determined by the sense of rotation of the neighboring oxygen octahedra (\mathbf{R}_{in} or \mathbf{R}_{out}). \mathbf{D} reads by the second order perturbation in the case of one electron per ion

$$\mathbf{D}_{Fe1,Fe2}^{(2)} = (4i/U)[b_{nn'}(Fe1-Fe2)C_{n'n}(Fe2-Fe1) - C_{nn'}(Fe1-Fe2)b_{n'n}(Fe2-Fe1)], \quad (5)$$

where U is the energy required to transfer one electron from one site to its nearest neighbor, a parameter similar to on-site Coulomb interaction in our *Ab initio* computation, and inversely proportional to \mathbf{D} . This is consistent with our calculated results that the absolute value of net magnetization is inversely proportional to the Hubbard parameter U . Magnetization does not reverse its direction in terms of the changing of the AFD displacement, especially when U is greater than the critical value of 2.9 eV, this indicates that in this case U is large enough to make DMI being disappeared. We have also calculated the band gap for different U corresponding to \mathbf{R}_{in} and \mathbf{R}_{out} , respectively. From Fig. 4, it can be seen that the curve becomes relatively flat when U reaches the critical value of 2.9 eV. Thereafter, we chose this value to describe the

electronic property in the following. It is worth mentioning that the band gap to \mathbf{R}_{in} is greater than to \mathbf{R}_{out} , indicating that the AFD motion corresponding to \mathbf{R}_{out} tend to reduce the crystal-field splitting, and consequently the band gap.

In order to analyze the rotation of magnetization under DMI, we have calculated the Orbital-resolved density of states(ODOS) for Fe1 and Fe2 corresponding to \mathbf{R}_{in} and \mathbf{R}_{out} in Fig.5, Fig. 6, Fig. 7, and Fig 8, respectively. Fig. 5 is the ODOS for Fe1 corresponding to \mathbf{R}_{in} rotational state. The vertical line indicates the Fermi level. All the states occupied in the valence band are spin-up electrons(majority spin as defined). It means the spin direction for Fe1 to \mathbf{R}_{in} is positive. Fig. 6 is the ODOS for Fe2 corresponding to \mathbf{R}_{in} rotational state. The vertical line indicates the Fermi level. All the states occupied in the valence band are spin-down electrons(majority spin as defined). It means the spin direction for Fe2 to \mathbf{R}_{in} is negative. Fig. 7 is the ODOS for Fe1 corresponding to \mathbf{R}_{out} rotational state. The vertical line indicates the Fermi level. All the states occupied in the valence band are spin-up electrons(majority spin as defined). It means the spin direction for Fe1 to \mathbf{R}_{out} is positive. Fig. 8 is the ODOS for Fe2 corresponding to \mathbf{R}_{out} rotational state. The vertical line indicates the Fermi level. All the states occupied in the valence band are spin-down electrons(majority spin as defined). It means the spin direction for Fe2 to \mathbf{R}_{out} is negative. Let us come back to Fig.3. In order to make the net magnetization reversed, the magnetic moment of Fe1 and Fe2 can rotate from the original direction corresponding to \mathbf{R}_{in} (Fig. 3(a)) either to the dashed line arrow(Fig.3 (b)) required greater energy barrier, or to the real line arrow required smaller energy barrier. From Fig. 5 to Fig.8, one can see that the spin-up electrons in the occupied valence band for Fe1 and the spin-down electrons in the occupied valence band for Fe2 do not change their in-built spin direction when rotational vector is changing from \mathbf{R}_{in} to \mathbf{R}_{out} . This confirms

that the spin direction of Fe1 and Fe2 only deviates slightly from the initial states to the final states as shown in the real line arrow in Fig.3 (b) corresponding to \mathbf{R}_{out} . It is worth pointing out that $d_{x^2-y^2}$ orbital for Fe1 and Fe2 is split from the doubly degenerate e_g states and tend to overlap with d_{xy} , d_{yz} , and d_{xz} orbitals in the triply degenerate t_{2g} states, indicating that the AFM DMI is mainly attributed to the e_g - e_g AFM interaction which is greater than the t_{2g} - t_{2g} AFM interaction.

4 Conclusion

Magnetization can be reversed by the altering sense of rotation of the oxygen octahedra in BiFeO₃ when U is smaller than the critical value of 2.9 eV, and the absolute value of magnetization is decreasing as U is ranging from 0 to 2.9 eV. Magnetization does not reverse with altered AFD displacement when U exceeds the critical value, indicating that the DMI is even prohibited in this case. The rotation of magnetization is fulfilled by slight deviation of magnetic moment of Fe1 and Fe2 around x axis rather than reversal of them.

References

- [1] M. Gajek, M. Bibes, S. Fusil, Nature Mater. 6(2007) 296.
- [2] Y. H. Chu, L. W. Martin, M. B. Holcomb, Nature Mater. 7(2008) 478.
- [3] G. Maugin, Phys.Rev.B 23(1981)4608.
- [4] H. Schmid, Ferroelectrics 162 (1994)317.
- [5] M. Fiebig, J.Phys.D:Appl. Phys. 38(2005)R123.

- [6] J. Wang, J. B. Neaton, H. Zheng, V. Nagarajan, S. B. Ogale, B. Liu, D. Viehland, V. Vaithyanathan, D. G. Schlom, U. V. Waghmare, N. A. Spaldin, K. M. Rabe, M. Wuttig, R. Ramesh, *Science* 299(2003)1719.
- [7] G. Catalan, J. F. Scott, *Adv. Mater.* 21(2009) 2463.
- [8] M. Cazayous, D. Malka, D. Lebeugle, D. Colson, *Appl. Phys. Lett.* 91(2007) 071910.
- [9] Manoj K. Singh, S. Dussan, W. Prellier, Ram s., Katiyar, *J. Mag. Mag. Mater.* 321(2009)1706.
- [10] Hongjian Feng, F. Liu, *Phys. Lett. A* 372(2008) 1904.
- [11] C. Ederer, N. A. Spaldin, *Phys. Rev. B* 71(2005)060401.
- [12] Hongjian Feng, F. Liu, *Chin.Phys. Lett.* 25(2008) 671.
- [13] The ABINIT code is a common project of the Universite Catholique de Louvain, Corning, Inc., and other contributors(URL <http://www.abinit.org>).
- [14] X. Gonze, J.-M. Beuken , R. Caracas, F. Detraux, M. Fuchs, G.-M. Rignanes, F. Jollet, M. Torrent, A. Roy, M. Mikami, P. Ghosez, J.-Y. Raty , D. C. Alan, *Comp. Mater. Sci.* 25(2002)478.
- [15] P. E. Blochl, *Phys. Rev. B* 50(1994)17953.
- [16] G. Kresse, D. Joubert, *Phys. Rev. B* 59(1999)1758.
- [17] V. I. Anisimov, J. Zaane, O. K. Andersen, *Phys. Rev. B* 44(1991)943.
- [18] V. I. Anisimov, I. V. Solovyev, M. A. Korotin, *Phys. Rev. B* 48(1993) 16929.
- [19] V. I. Anisimov, F. Aryasetiawanz, A. I. Lichtenstein, *J. Phys.: Condens. Matter.* 9(1997)767.
- [20] C. Ederer., C. J. Fennie, *J. Phys. Condens. Matter.* 20(2008) 434219
- [21] P. W. Anderson, *Phys. Rev.* 115(1959)2.

[22] T. Moriya, Phys. Rev. Lett. 4(1960)228.

[23] T. Moriya, Phys. Rev. 120(1960)91.

Table 1

Magnetization per unit cell with respect to different value of U and J .

$U(eV)$	0		0.5		0.8		1		1	
$J(eV)$	0		0.5		0.8		1		0	
	\mathbf{R}_{in}	\mathbf{R}_{out}	\mathbf{R}_{in}	\mathbf{R}_{out}	\mathbf{R}_{in}	\mathbf{R}_{out}	\mathbf{R}_{in}	\mathbf{R}_{out}	\mathbf{R}_{in}	\mathbf{R}_{out}
$M_x(\mu_B)$	0.0000	0.0000	0.0000	0.0000	0.0000	0.0000	0.0000	0.0000	0.0000	0.0000
$M_y(\mu_B)$	0.4259	-0.0812	0.4259	-0.0812	0.4259	-0.0812	0.4259	-0.0812	0.0351	-0.0679
$M_z(\mu_B)$	-0.1013	0.0000	-0.1013	0.0000	-0.1013	0.0000	-0.1013	0.0000	-0.0493	0.0056
$U(eV)$	2		2.5		2.8		2.9		3.4	
$J(eV)$	0		0		0		0		0.5	
	\mathbf{R}_{in}	\mathbf{R}_{out}	\mathbf{R}_{in}	\mathbf{R}_{out}	\mathbf{R}_{in}	\mathbf{R}_{out}	\mathbf{R}_{in}	\mathbf{R}_{out}	\mathbf{R}_{in}	\mathbf{R}_{out}
$M_x(\mu_B)$	0.0000	0.0000	0.0000	0.0000	0.0000	0.0000	0.0000	0.0000	0.0000	0.0000
$M_y(\mu_B)$	0.0416	-0.0337	0.0325	-0.0251	0.0365	-0.0188	0.0313	-0.0176	0.0313	-0.0176
$M_z(\mu_B)$	-0.0408	0.0108	-0.0366	0.0147	-0.0431	0.017	-0.0406	0.0168	-0.0406	0.0168
$U(eV)$	3.7		3		4		5		6	
$J(eV)$	0.8		0		0		0		0	
	\mathbf{R}_{in}	\mathbf{R}_{out}	\mathbf{R}_{in}	\mathbf{R}_{out}	\mathbf{R}_{in}	\mathbf{R}_{out}	\mathbf{R}_{in}	\mathbf{R}_{out}	\mathbf{R}_{in}	\mathbf{R}_{out}
$M_x(\mu_B)$	0.0000	0.0000	0.0000	0.0000	0.0000	0.0000	0.0000	0.0000	0.0000	0.0000
$M_y(\mu_B)$	0.0313	-0.0176	0.0237	0.0012	0.0172	0.0033	0.0176	0.0085	0.0178	0.0111
$M_z(\mu_B)$	-0.0406	0.0168	-0.0283	-0.0049	-0.0249	-0.0055	-0.0186	-0.0053	-0.0157	-0.0025

Figure captions:

Fig.1 The rotational vectors of the AFD distortions in BiFeO_3 . The shaded cage denote the oxygen octahedra, and Fe is inside the cage.

Fig.2 AFM vectors with respect to U .

Fig.3 Schematic diagram for the coupling between the rotation of oxygen octahedra and the resulting magnetization in unit cell in BiFeO_3 . The arrow denote the direction of magnetization.

Fig. 4 Band gap for \mathbf{R}_{in} and \mathbf{R}_{out} with respect to U .

Fig. 5 ODOS for Fe1 $d_{xy}, d_{yz}, d_{z^2}, d_{xz}$, and $d_{x^2-y^2}$ orbitals to \mathbf{R}_{in} .

Fig. 6 ODOS for Fe2 $d_{xy}, d_{yz}, d_{z^2}, d_{xz}$, and $d_{x^2-y^2}$ orbitals to \mathbf{R}_{in} .

Fig. 7 ODOS for Fe1 $d_{xy}, d_{yz}, d_{z^2}, d_{xz}$, and $d_{x^2-y^2}$ orbitals to \mathbf{R}_{out} .

Fig. 8 ODOS for Fe2 $d_{xy}, d_{yz}, d_{z^2}, d_{xz}$, and $d_{x^2-y^2}$ orbitals to \mathbf{R}_{out} .

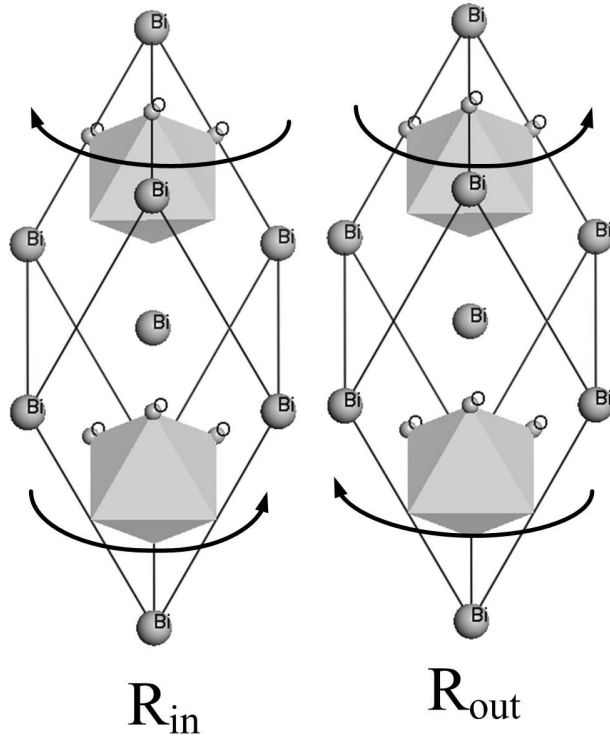


Fig. 1. The rotational vectors of the AFD distortions in BiFeO_3 . The shaded cage denote the oxygen octahedra, and Fe is inside the cage.

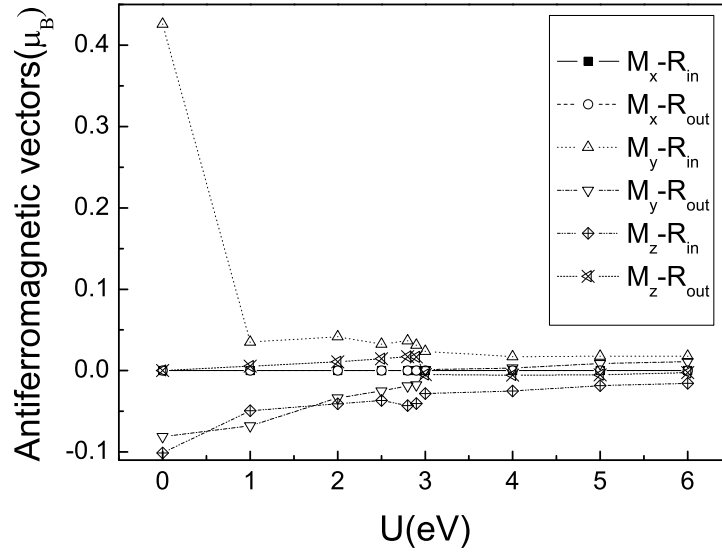


Fig. 2. AFM vectors with respect to U .

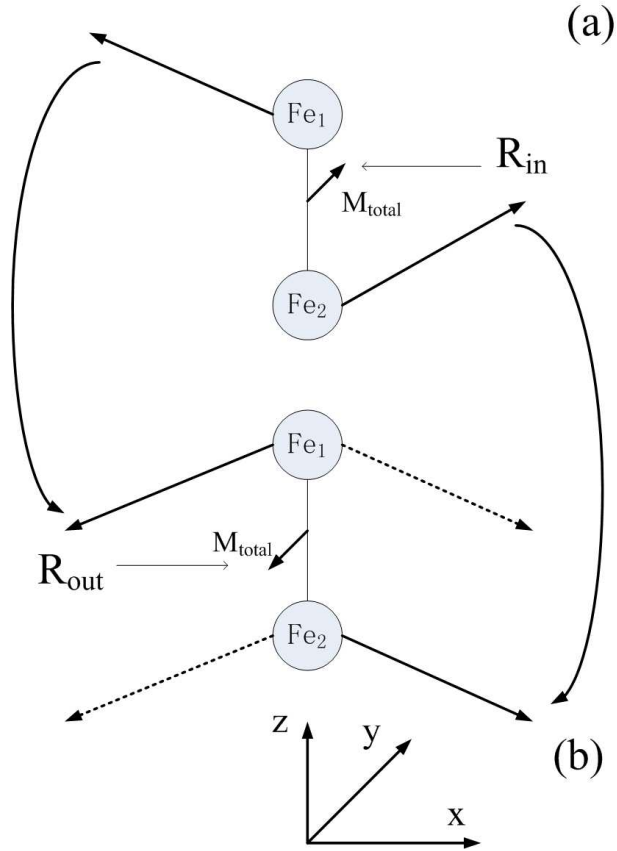


Fig. 3. Schematic diagram for the coupling between the rotation of oxygen octahedra and the resulting magnetization in unit cell in BiFeO_3 . The arrow denote the direction of magnetization.

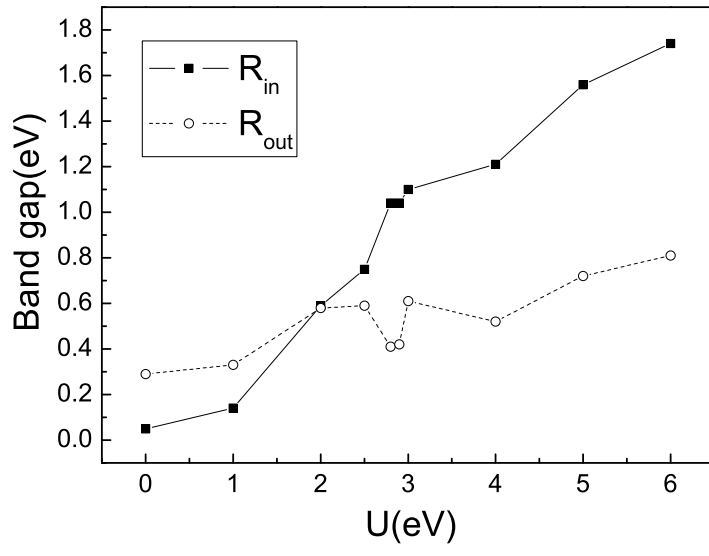


Fig. 4. Band gap for R_{in} and R_{out} with respect to U .

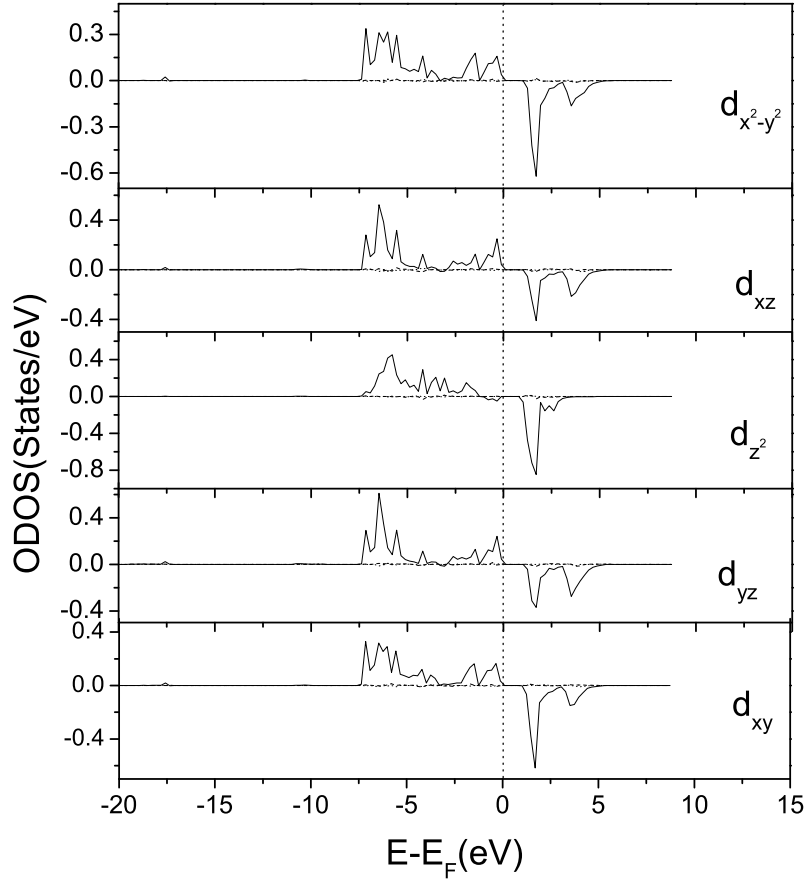


Fig. 5. ODOS for Fe1 d_{xy} , d_{yz} , d_{z^2} , d_{xz} , and $d_{x^2-y^2}$ orbitals to \mathbf{R}_{in} .

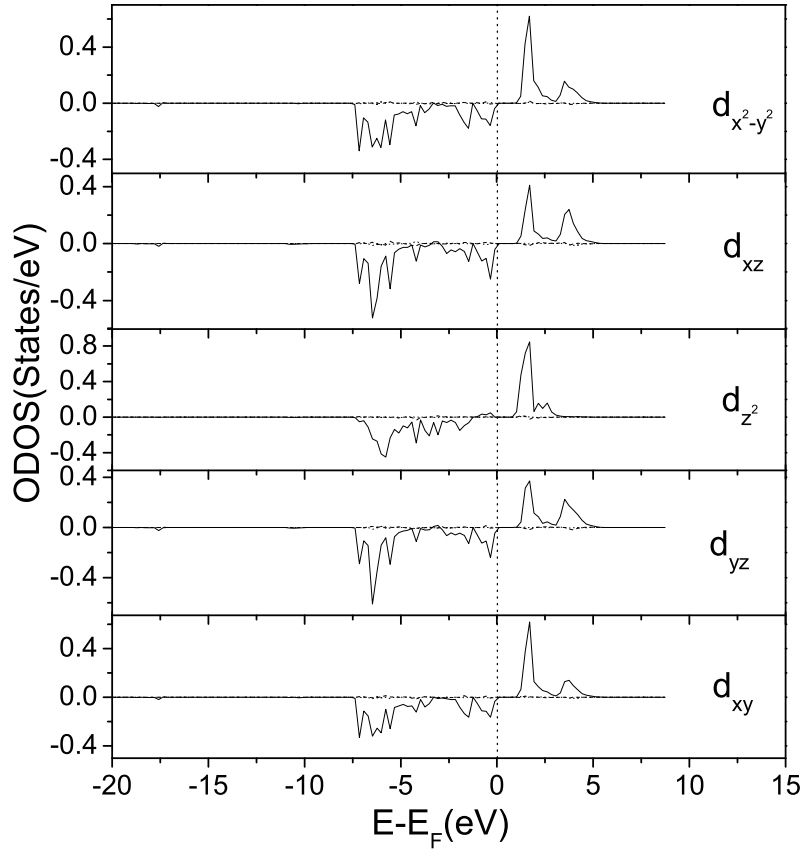


Fig. 6. ODOS for Fe2 d_{xy} , d_{yz} , d_{z^2} , d_{xz} , and $d_{x^2-y^2}$ orbitals to \mathbf{R}_{in} .

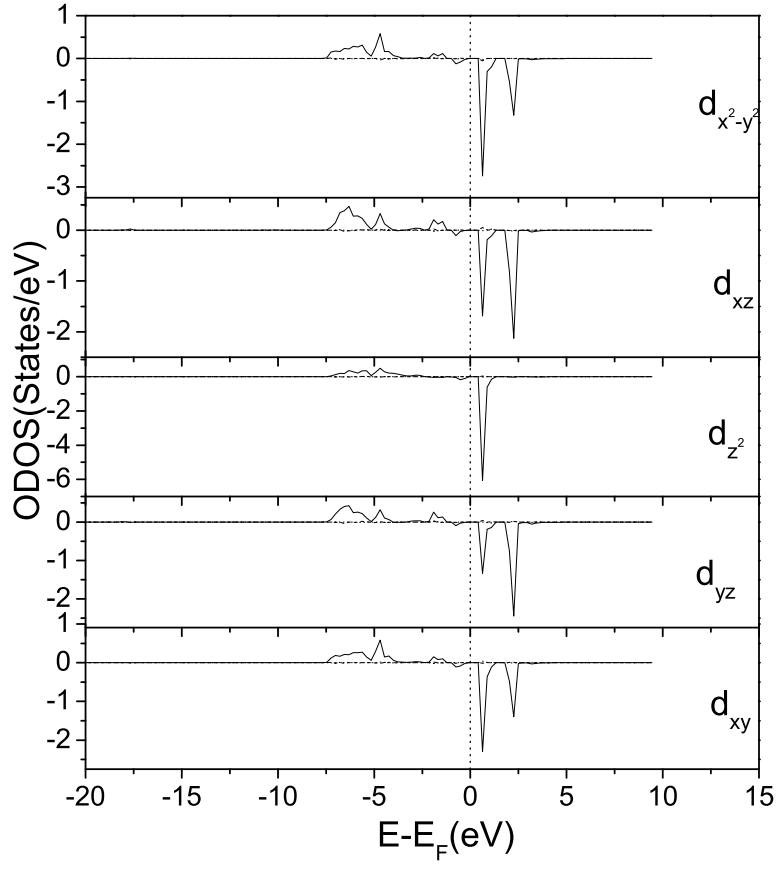


Fig. 7. ODOS for Fe1 d_{xy} , d_{yz} , d_{z^2} , d_{xz} , and $d_{x^2-y^2}$ orbitals to \mathbf{R}_{out} .

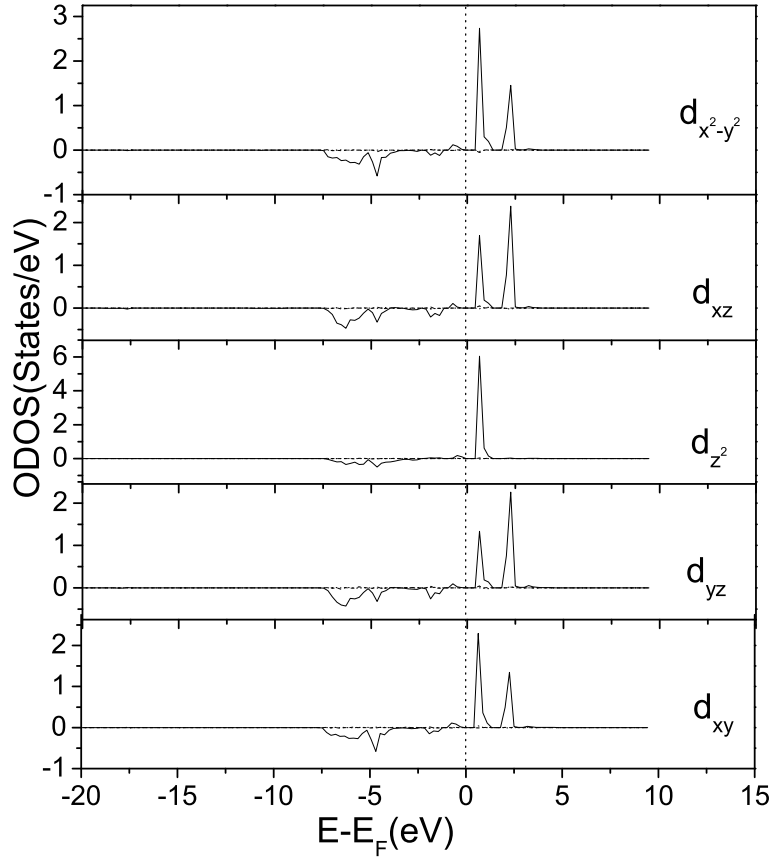


Fig. 8. ODOS for Fe2 d_{xy} , d_{yz} , d_{z^2} , d_{xz} , and $d_{x^2-y^2}$ orbitals to \mathbf{R}_{out} .